

Holographic Wavefront Sensor

Geoff Andersen

US Air Force Academy

Fassil Ghebremichael and Ken Gurley

Lockheed Martin Missiles and Fire Control

1. ABSTRACT

There are several different types of wavefront sensors that can be used to measure the phase of an input beam. While they have widely varying modes of operation, they all require some computational overhead in order to deconstruct the phase from an optical measurement which reduces the sensing speed. Furthermore, zonal detection methods, such as the Shack-Hartmann wavefront sensor (SHWFS) are not well suited to temporal changes in pupil obscuration such as can occur with scintillation. Here we present a modal detector that incorporates a multiplexed hologram to give a full description of wavefront error without the need for any calculations.

2. INTRODUCTION

Wavefront sensors are a critical component of adaptive optics systems. There are many different types such as interferometric, Shack-Hartmann (SHWFS) and curvature sensors, each with their own advantages and trade-offs [1-8]. However, one over-riding similarity is that they all have limited speed due to finite processing capabilities. For this reason, even the most advanced wavefront systems are only capable of 10kHz updates. Worse still, these wavefront sensors are far from compact. Here we present a holographic wavefront system in which a multiplexed hologram is recorded with all of the expected aberration modes. An input beam incident on this hologram will be diffracted into multiple pairs of output beams – a single pair for each mode. By measuring the relative power in each beam we can directly measure the amplitude of that particular mode. In essence this holographic wavefront sensor (HWFS) is acting as an all-optical parallel processing unit. With the use of position sensing devices (PSDs) we can fully characterize any wavefront at MHz rates. Added to this is the benefit of a sensor that is modal rather than zonal and is thus relatively insensitive to strong scintillation.

3. HOLOGRAPHIC WAVEFRONT SENSOR

For our holographic wavefront sensor we are choosing the standard Zernike formalism for describing aberration modes over a circular aperture [2, 8-12]. The choice of basis set is not critical so long as the modes are orthogonal. In simple terms the Zernike polynomials can be described as a sum of modes (Z_i) with corresponding amplitudes (A_i):

$$W(\rho, \theta) = \sum_{i=1}^{\infty} A_i Z_i \quad (1)$$

Our holographic wavefront sensor is best understood in how it can be created to measure the amplitude of a single aberration (Z_i), and the holograms in question will be created optically. The first hologram is constructed by using an object beam consisting of the minimum expected amplitude of the aberration ($A_{min}Z_i$) and a reference beam consisting of a diffraction limited beam focused to a distant point A as shown in Fig. 1. A second hologram is then recorded on the same piece of film using the maximum amplitude of the aberration ($A_{max}Z_i$) and a reference beam focused to a different point B.

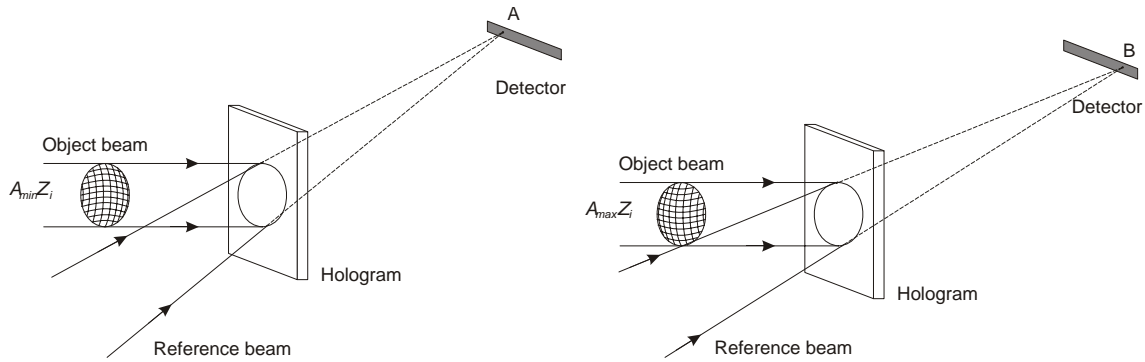


Fig. 1: The minimum (left) and maximum (right) of a particular aberration component is recorded along with a reference beam focused to a different point on a distant screen.

On reconstruction, if an object beam with an arbitrary amplitude (A_i) of the recorded aberration is incident on the multiplexed hologram ($A_{min} < A_i < A_{max}$) there will be two diffracted beams focusing to locations A and B on a distant screen (Fig. 2). The relative power of the two focal spots is directly proportional to the recorded amplitudes A_{min} and A_{max} . In effect, these extreme amplitude values represent “goalposts” between which an accurate measure of amplitude can be obtained. Given a simple sensor such as a position sensing device (PSD), a fast measure of this relative power can be accomplished without the need for any computations.

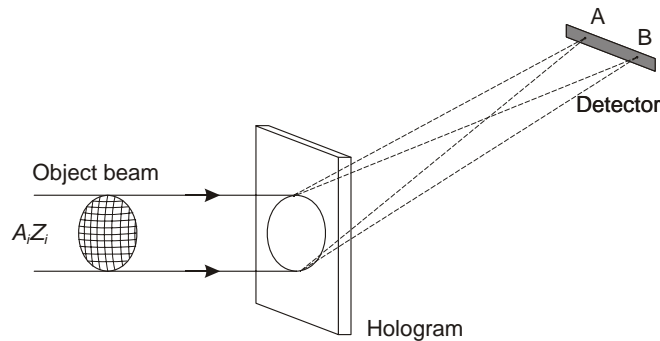


Fig. 2: On reconstruction two focused beams are diffracted from the hologram. The relative intensities of the two focal spots at the detector give a measure of the amplitude of the mode.

A more general wavefront sensor would consist of a multiplexed hologram having many more aberrations (modes) recorded in the same medium. In this case, each mode would still require a pair of holograms and each mode would be separated out spatially to separate PSDs as shown in Fig. 3.

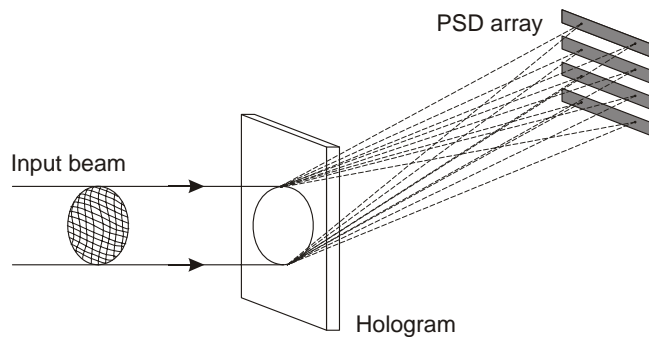


Fig. 3: Multiple aberrations can be sensed by multiplexing each in the hologram. A spatial separation of the beams is required to direct the spots onto different PSDs.

In any multiplexed hologram there is the issue of cross-talk to be considered. In this case there are two types of cross-talk: intermodal and intramodal. The first is actually required for the holographic wavefront to operate correctly. Without intermodal cross-talk there would not be two focal spots which are used to measure the amplitude. Intramodal cross-talk is more of an issue and it was necessary to show that the presence of one aberration does not affect the amplitude measurement of another. Our modeling shows that this has a negligible effect on the performance of the system. In one model we created a hologram sensitive to $\pm 1.2\lambda$ of astigmatism. When we introduced varying amounts of coma, there was little noticeable effect on the measured output in the astigmatism channel as shown in Fig. 4.

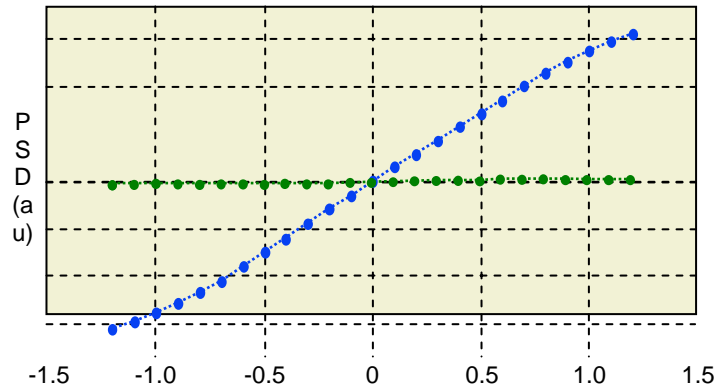


Fig. 4: A graph showing the PSD output at the “astigmatism” channel with varying input amplitudes of astigmatism (blue) and coma (green).

The advantage of the holographic wavefront sensor is that a full description of any wavefront can be made without any computations. Using PSD detectors, speeds of up to MHz rates are possible, while being considerably more compact than other types of WFS. A further benefit of this method is that the sensing is modal instead of zonal as in the case of the SHWFS. In the case of scintillation where intensity variations can lead to regions of zero intensity on the input beam zonal detectors will be unable to create a full wavefront phase map, but a modal detector is largely unaffected.

The trade-offs for the HWFS over competing methods are twofold. Firstly since the hologram is dispersive, the HWFS is not suitable for broadband input beams. For this reason, the holographic wavefront sensor is limited to narrowband sources, and a new hologram is required for each different wavelength used. Secondly, since a single input beams is divided up amongst multiple output beams, there will ultimately be some limit on the number of holograms that can be multiplexed before the detection limit is reached for a given source and PSD combination.

Perhaps the most ideal application for the holographic wavefront sensor is in conjunction with the Airborne Laser. In this case both high speed and insensitivity to scintillation are critical for success, while the requirement of a narrowband (laser) input beam and limitation of moderate to high light levels are not particularly restrictive.

4. EXPERIMENT

In order to assess the performance of the holographic wavefront sensor, we first constructed a hologram to measure the amplitude of a single aberration. In this case we chose defocus due to its ability to be easily created in the lab. We tried two different types of hologram in our experiments: optically constructed in photographic media (silver halide film) and computer generated in etched fused silica. Both methods produced similar results and while the silver halide approach was simple and inexpensive, it is unlikely to be suitable for higher order terms as this would require generating high quality “pure” optical constructions of each aberration which may be difficult. Instead, we are concentrating on computer generated methods for future experiments.

In our experiment we chose to record ± 1.2 waves of defocus in a computer generated hologram. The hologram had a 15mm circular cross-section consisting of a 7500x7500 pixel array of $2\mu\text{m}$ pixels. The surface relief holograms were

created using photolithographic techniques to give 3-bit (8 level) etched patterns. The focal length (derived from the “reference” beam used in calculating the patterns) was 250mm, with a 35mm off-axis distance to separate the diffracted spots out from the undiffracted zero order. In measuring the power, the signal to noise was improved by using two 20 μ m pinholes located the focal planes. For this test optical power meters were used instead of the suggested linear PSDs, but the recorded values were combined to simulate the result expected from a PSD. By varying the input defocus, we measured the output values as shown in Fig. 5.

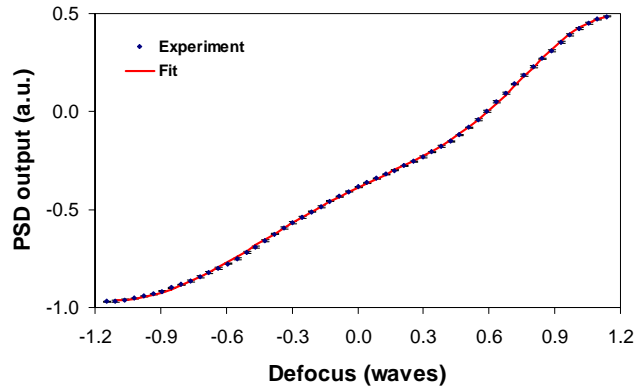


Fig. 5: A graph of the simulated PSD output against defocus input.

The fit provided is simply the sum of two Gaussian curves as derived from our theoretical modeling of the system. The results of this experiment indicate that defocus could be measured over the design range of $\pm 1.2\lambda$ to a precision of $\lambda/90$.

5. MORE ABERRATIONS

We are currently improving the system to include more aberrations. In principle, this is a simple matter of making the calculations necessary to encode the hologram with more holograms. In practice, however, the method for multiplexing the holograms on a single diffractive element is more complex. For example, a randomized interpolation of the pixels will lead to a large amount of diffusion characteristic of a random distribution of 2mm pixels with little light diffracting into our focal spots. Meanwhile, a regular interpolation leads to a loss of light in creating bright higher-order replica patterns of our focal spots. We are currently investigating several solutions to this problem as we progress to a HWFS for 8 Zernike terms.

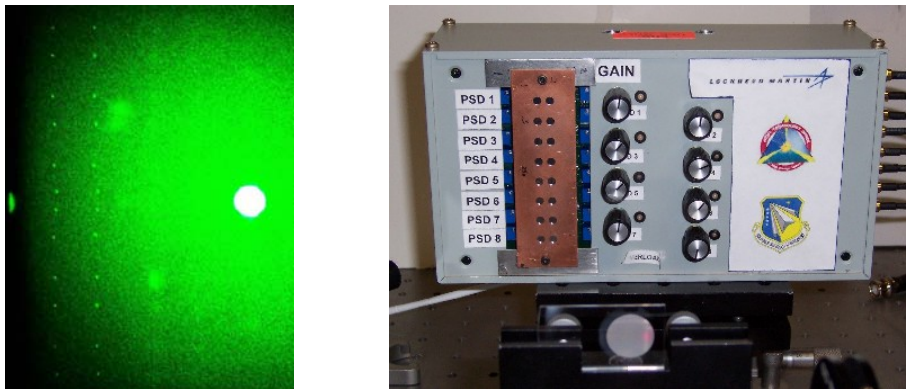


Fig. 6: The spot pattern output from our etched CGH (left). The PSD detector array sits behind the pinhole array in our electronics system (right).

As the design of the hologram is optimized we have also constructed a detector capable of measuring the power in the focal spots at high speeds. For this we are using an array of 8 linear PSDs mounted in a single unit. Our

electronics will permit detection of light levels down to nanoWatts at speeds of up to 100kHz. This is approximately 10 times faster than currently possible with state-of-the-art Shack-Hartmann systems.

6. CONCLUSION

We have introduced a holographic wavefront sensor capable of fast, computer-free characterization of input wavefronts using a simple, compact system. This modal sensor should be ideal for operation with the Airborne Laser as it is largely insensitive to scintillation and can be designed to operate at MHz rates. Our experiments have demonstrated it behaves as expected for a single aberration and we are now experimenting with adding higher order aberrations.

ACKNOWLEDGEMENTS

We would like to acknowledge support for this project from the Joint Technology Office (JTO) and the Air Force Office of Scientific Research (AFOSR).

REFERENCES

1. J. M. Geary, "Introduction to Wavefront Sensors", SPIE Press, Vol. TT18 (1995).
2. D. Malacara, "Optical Shop Testing 2nd Ed.," Wiley-Interscience Press (1992).
3. J. Son et al., "Shack-Hartmann wavefront sensor with holographic memory," *Opt. Eng.* **42** 3389-3398 (2003).
4. J. Rha et al., "Reconfigurable Shack-Hartmann wavefront sensor," *Opt. Eng.* **43** 251-256 (2004).
5. R. Clare and R. Lane, "Phase retrieval from subdivision of the focal plane with a lenslet array," *Appl. Opt.* **43** 4080-4087 (2004).
6. F. Roddier, "Curvature sensing and compensation: a new concept in adaptive optics," *Appl. Opt.* **27** 1223-1225 (1988).
7. P. Hariharan, "Optical Holography 2nd Ed.," Cambridge Press (1996).
8. R. Dyson, "Principles of Adaptive Optics 2nd Ed.," Academic Press (1998).
9. F. Roddier, "Adaptive Optics in Astronomy," Cambridge Press (1999).
10. R. J. Noll, "Zernike polynomials in atmospheric turbulence," *J. Opt. Soc. Am.* **66** 207-211 (1976).
11. S. Restaino et al., "Analysis of the Naval Observatory Flagstaff Station 1-m telescope using annular Zernike polynomials," *Appl. Opt.* **42** 2491-2495 (2003).
12. C. Sheppard et al., "Zernike expansion of separable function of Cartesian coordinates," *Appl. Opt.* **43** 3963-3966 (2004).